PROCEEDINGS OF SCIENCE

# *Maser astrometry (Review)*

**Nobuyuki Sakai**[a,*]

[a] *National Astronomical Research Institute of Thailand (Public Organization), 260 Moo 4, T. Donkaew, A. Maerim, Chiangmai, 50180 Thailand*

*E-mail:* nobuyuki@narit.or.th

We summarize the review talk of "Maser astrometry" which was given in the 15th EVN (European VLBI Network) Symposium. The basics of VLBI astrometry is introduced in section 1. In section 2, we briefly introduce the background and context of the contributed talks given in the session "Techniques 1". In section 3, we review scientific achievements with maser astrometry, which are (1) the Galactic structure and (2) an accretion event in the high-mass protostar G358.93−0.03-MM1. The VLBA BeSSeL and VERA projects have compiled more than 200 VLBI astrometric results, which reveals that the Milky Way is a barred spiral with four major arms and secondary arms. The results update Galactic constants to be ($R_0$, $\Theta_0$) = (8.15±0.15 kpc, 236±7 km s$^{-1}$). The rotation velocity of the LSR, $\Theta_0$, is larger than the IAU 1985 recommendation value (i.e., 220 km s$^{-1}$). It indicates that the Milky Way is ∼10-30% heavier than previously thought, since the total mass of the Milky Way scales as $(\Theta_0)^3$ in the NFW dark halo potential. The "episodic accretion" theory of high-mass star formation was observationally confirmed for G358.93−0.03-MM1 by the Maser Monitoring Organization (M2O) operating several radio telescopes in the world. The proper motion of G358.93−0.03-MM1 was measured to be 1-2 mas (milliarcsecond) Day$^{-1}$ (11,700-23,400 km s$^{-1}$ at $d$ = 6.75 kpc) by VLBI observations of 6.7 GHz methanol masers. Such a fast motion could be explained under the hypothesis of an accretion event in which enhanced far-infrared radiation drives the production of the methanol masers. Last of all, we introduce future prospects in section 4.

*15th European VLBI Network Mini-Symposium and Users' Meeting (EVN2022)*
*11-15 July 2022*
*University College Cork, Ireland*

*Speaker





PoS(EVN2022)060

## 1. Basics of VLBI astrometry

VLBI position measurements using phase referencing are the most accurate of radio methods [43]. Accurate position measurements allow one to measure the trigonometric parallax and proper motion for astronomical objects such as masers, pulsars, Active Galactic Nuclei, and radio stars. The trigonometric parallax is a projection of Earth's orbit, while the proper motion is caused due both to the actual relative motions of the Sun and the target.

Here, we briefly introduce the basics of VLBI astrometry. More details of VLBI astrometry are well summarized in two review papers which are Reid & Honma [32] and Rioja & Dodson [37].

### 1.1 The history of parallax measurements

Please keep in mind that the parallax is always a "*relative*" position measurement. Hipparchus estimated the distance to the moon by measuring the parallax of the edge of the moon in 129 BC[1]. Bessel [3] measured the first stellar parallax for 61 Cygni relative to a distant star. Reid & Menten [33] reanalyzed the data used by Bessel [3]. The Hipparcos satellite was launched in 1987 by the European Space Agency (ESA) to measure stellar parallaxes within 100 pc from the Sun [28]. While the original Hipparcos catalog was published by ESA [9], van Leeuwen [44] reanalyzed the catalog. The revised Hipparcos catalog contains ~120,000 astrometric results. Recently, VLBI and *Gaia* astrometric projects have been measuring trigonometric parallaxes of Galactic objects with an accuracy of 10 microarcsecond ($\mu$as) level, which allows us to measure a distance of 10 kpc with 10% accuracy. The history of parallax measurements is summarized in Fig. 1.

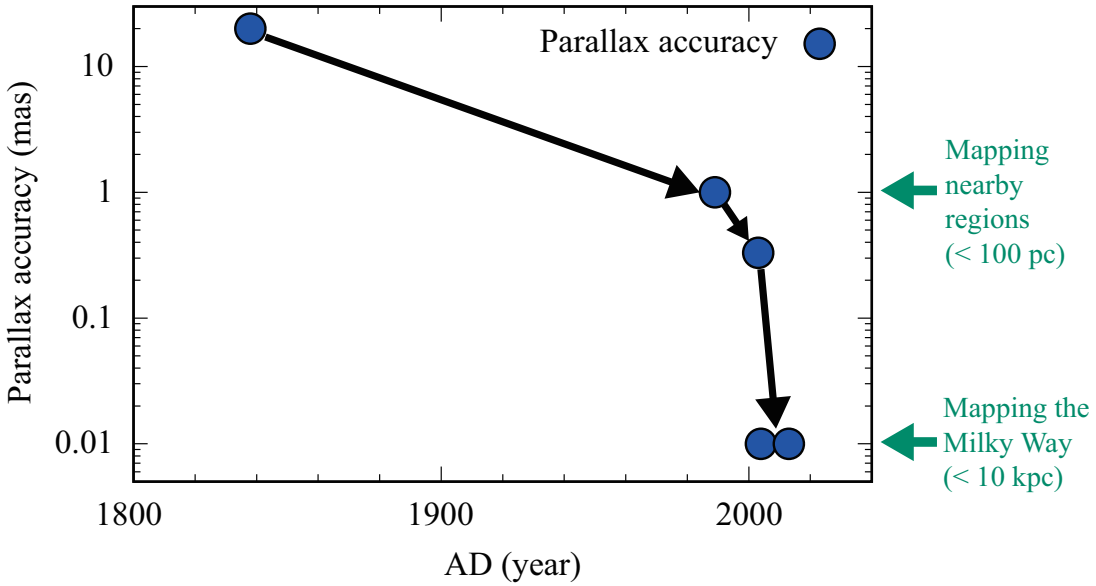


**Figure 1:** Parallax accuracy is shown as a function of time. Individual data references are listed in chronological order: (1) Bessel [3]; (2) Perryman [28]; (3) Vlemmings et al. [46]; (4) Hirota et al. [13], Honma et al. [14] (5) Gaia Collaboration et al. [10].

[1]See a NASA's web page: https://pwg.gsfc.nasa.gov/stargaze/Shipparc.htm

### 1.2 "1-2-1" schedule

The trigonometric parallax can be separated from the proper motion with well selected observations. For example, Sato et al. [40] chose four optimal epochs in which to sample only the parallax peaks of Right Ascension (R.A.) for a 22 GHz water maser spot associated with the massive star-forming region W51 Main/South, since the parallax amplitude of R.A. was about twice as large as that of declination. The two middle epochs were chosen close to each other and near one parallax peak, which is called *"1-2-1" schedule*. The two middle epochs are needed for symmetry and to obtain similar accuracy for the parallax maximum and minimum. Approximate formulae for accuracies for the parallax and proper motion are shown in the Appendix (see 5).

### 1.3 The Lutz-Kelker bias

If the trigonometric parallax, $\pi$, is well less than 1 radian (i.e., $\pi \ll 1$), the distance of an astronomical object, $d$, can be measured by inverting the trigonometric parallax as

$$d = \frac{1\ [\mathrm{AU}]}{\tan(\pi)}$$

and

$$d\ [\mathrm{pc}] \simeq \frac{1}{\pi\ [\mathrm{arcsecond}]} \tag{1}$$

The unit of parsec is defined based on Eq. 1. Since the distance determination via the trigonometric parallax measurement is nonlinear conversion, a bias effect on Eq. 1 has been discussed (e.g., 2; 21). In Eq. 1 the full probability density function of the distance is asymmetry and can have a large "tail" toward large distances when the fractional parallax error is larger than 20%, which is called the "Lutz-Kelker bias". Bailer-Jones [2] recommended using a simple prior which decreases asymptotically to zero at infinite distance when determining the distance via the trigonometric parallax measurement.

### 1.4 Error sources on relative VLBI astrometry

In relative VLBI astrometry, one observes the target and reference at nearly the same time and nearly the same position on the sky. We difference the observed delays (phases) between the pair of sources as

$$\begin{aligned}\Delta\tau\ &= (\tau_{\mathrm{geo},1} - \tau_{\mathrm{geo},2}) + (\tau_{\mathrm{tropo},1} - \tau_{\mathrm{tropo},2}) + (\tau_{\mathrm{iono},1} - \tau_{\mathrm{iono},2}) + (\tau_{\mathrm{ant},1} - \tau_{\mathrm{ant},2}) \\ &\quad + (\tau_{\mathrm{inst},1} - \tau_{\mathrm{inst},2}) + (\tau_{\mathrm{struc},1} - \tau_{\mathrm{struc},2}) + (\tau_{\mathrm{therm},1} - \tau_{\mathrm{therm},2}).\end{aligned} \tag{2}$$

Here, subscripts 1 and 2 denote the observed quantities for the target and reference sources, respectively. This type of observation is referred to as "phase referencing" (i.e., Eq. 2). The geometric delay ($\tau_{\mathrm{geo}}$) is due to the position of a source. Delays originate in the propagation of the signal through the troposphere ($\tau_{\mathrm{tropo}}$) and ionosphere ($\tau_{\mathrm{iono}}$). The error on the location of an antenna produces the delay ($\tau_{\mathrm{ant}}$). The instrumental delay ($\tau_{\mathrm{inst}}$) originates in the telescope or electronics. Unmodeled source structure produces the delay ($\tau_{\mathrm{struc}}$). The uncertainty of the measured delay originates in thermal errors ($\tau_{\mathrm{therm}}$). We should minimize all the delays explained above for high

precision astrometry, except for the geometric delay.

Four terms in Eq. 2, ($\tau_{\rm tropo}$, $\tau_{\rm iono}$, $\tau_{\rm ant}$, $\tau_{\rm inst}$), are antenna-based quantities (i.e., delays measured at each antenna site), which are generally similar toward the target and reference lines of sight for small source separations. Thus, the four terms can be reduced by phase referencing. The effect of source structure (i.e., $\tau_{\rm struc}$) is a baseline based quantity, and it can be modeled in data reduction using the technique of iterative self-calibration.

The error budget on Eq. 2 depends on an observing frequency. The residual of tropospheric delay measurements is dominant at a frequency ($\nu$) larger than 10 GHz, whereas that of ionospheric delay measurements is dominant at $\nu < 10$ GHz [32].

### 1.5 Single-epoch position accuracy in relative VLBI astrometry

As explained above, the dominant error source on relative VLBI astrometry originates in the tropospheric delay at a frequency larger than 10 GHz. In other words, the position accuracy in relative VLBI astrometry is limited by a systematic error (i.e., troposphere and/or ionosphere). The tropospheric delay can be measured with GPS and/or weather information (i.e., atmospheric pressure, temperature, and relative humidity). Nagayama et al. [25] compared a tropospheric zenith delay measured with GPS to that with JMA (Japan Meteorological Agency meso-scale analysis data), and concluded that both methods can calibrate the tropospheric zenith delay within an accuracy of ~2 cm in the units of $c\tau_{\rm trop}$ where the $c$ is the speed of light.

A single-epoch position error caused by the residual of tropospheric delay was shown by Nagayama et al. [26] as

$$\begin{aligned}\Delta\theta_{\rm tro} &\approx \frac{c\Delta\tau_{\rm tro}}{D}\Delta{\rm secZ} \\ &= 30\left(\frac{c\Delta\tau_{\rm tro}}{2\ {\rm cm}}\right)\left(\frac{2400\ {\rm km}}{D}\right)\left(\frac{\Delta{\rm sec}ZA}{1\ {\rm deg}}\right)\ [\mu{\rm as}]\end{aligned}$$

where $c$ is the speed of light, $\tau_{\rm tro}$ the tropospheric delay residual, $D$ the baseline length of a VLBI array, and $ZA$ is the antenna zenith angle. Note that $\Delta{\rm sec}ZA$ is a difference between ${\rm sec}ZA$ values of the target and reference sources. While $\Delta{\rm sec}ZA = {\rm sec}ZA\ {\rm tan}ZA\ \Delta ZA = 3.5\ \Delta ZA$ for $ZA = 60°$, $\Delta{\rm sec}ZA = 8.0\ \Delta ZA$ for $ZA = 70°$. Thus, astrometric data with $ZA < 60°$ should be used for a better position accuracy.

## 2. Contributed talks in the session "Techniques 1"

Followed by this review talk in the session "Techniques 1", three contributed talks were given[2]. We briefly introduce the three contributed talks here, while we recommend readers to see individual proceedings of three speakers.

[2]See individual presentation files at https://www.ucc.ie/en/evn2022/scientificprogramme/

Dr. Hagiwara introduced the development of ultra-wide band polarimetry with a recording rate of 16 Gbps for the VERA (VLBI Exprolation of Radio Astrometry) array. This enables us to detect a polarized intensity of 1 mJy. A short term goal of this project is to conduct joint polarimetric observations with VERA and the KVN (Korean VLBI Network) at 22 and 43 GHz, while a long term goal of this project is to expand this activity into the EAVN (East Asian VLBI Network) and Global-VLBI alliance. Science cases with the ultra-wide band polarimetry cover "Larger Faraday Rotation measure in plasma jest", "Long-term monitoring of magnetic fields in the vicinity of a super massive black hole", and "magnetic fields of stellar envelopes in late-type stars".

Dr. Hyland introduced the technique "inverse MultiView (iMV; 17, 18)", which can be used for ionospheric calibration which is a dominant error source on VLBI position measurements at a frequency less than 10 GHz. The iMV technique is the combination of inverse Phase Referencing (iPR) and MultiView (MV) techniques, which allows one to achieve single-epoch astrometric accuracies near 20 microarcsecond ($\mu$as) for target-reference quasar separations up to $\sim 7^\circ$ at 8.6 GHz. A difference between the MV and iMV techniques is an observing sequence as

$$C_1,\ C_2,\ C_3,\ T,\ C_1 \ldots. \text{ (MultiView)}$$
and
$$T,\ C_1,\ T,\ C_2,\ T, \ldots,\ C_N,\ T,\ C_1 \ldots \text{ (inverse MultiView)}$$

where $T$ is the target and $C$ denotes $N$ quasars. While multiple quasars and the target source should be observed within the coherence time of the atmosphere in the case of MV, iMV only requires that adjacent observations of the target source should be observed within the coherence time. By applying the iMV calibration for 6.7 GHz methanol masers associated with the star-forming regions G232.62+00.99 and G323.74–00.26, Hyland et al. [18] succeeded in measuring trigonometric parallaxes of these sources to be 0.610±0.011 milliarcsecond (mas) and 0.364±0.009 (mas), respectively.

Dr. Boven introduced the progress of their project on VLBI "MultiView" astrometry of Radio Stars. Different types of stars show radio emission whose mechanisms are (1) free-free radiation mostly come from stellar outflows and chromosphere, and (2) synchrotron/gyrosynchrotron radiation generated in stellar flares [49]. Xu et al. [47] compared the parallaxes of radio stars from VLBI astrometry to those from *Gaia* (optical) astrometry, which allowed them to determine a zero-point parallax of −75±29 microarcsecond ($\mu$as) for *Gaia* DR2. Between the June of 2020 and the March of 2021, Dr. Boven conducted three-epochs EVN (Europian VLBI Network) astrometry for the binary system Ross 867 (M4.5V) and Ross 868 (M3.5V). However, only Ross 867 was detected in the observations, which is consistent with a previous result of [29]. Boven et al. have conducted this kind of observation for other M dwarfs, which allows them to compare the emission region of optical to that of radio for the M dwarfs. Also, it can allow them to measure the polarization and variability of the M dwarfs.

## 3. Scientific achievements with maser astrometry

### 3.1 The Galactic structure

The VERA (VLBI Exploration of Radio Astrometry) and BeSSeL (Bar and Spiral Structure Legacy Survey) projects have compiled more than 200 trigonometric parallaxes of Galactic masers (i.e., 6.7/12 GHz methanol masers; 22 GHz water masers; 43 GHz silicon monoxide masers) for making a 3D map of the Milky Way (see 36; 45). Based on the 200 parallax results, the Milky Way is recognized as a four-arm spiral galaxy with extra arm segments and spurs (see Fig. 2).

The VERA is a Japanese VLBI project[4] while the BeSSeL is the largest VLBA program which has spent 3500 hours of VLBA time[5]. The 200 parallax results combined with proper motion and line-of-sight velocity results can be used to determine Galactic fundamental parameters including Galactic constants which are $R_0$ and $\Theta_0$. The former is the distance to the Galactic center while the latter is the rotation velocity of the LSR (Local Standard of Rest). Determinations of ($R_0$, $\Theta_0$) with maser astrometry and other methods are summarized in Fig. 3.

Figure 3 shows that statistical errors of $R_0$ and $\Theta_0$ are decreased with increasing the number of VLBI astrometric results (i.e., parallax and proper motion results). Also, $R_0$ = 8.15±0.15 kpc of [36] is smaller than the IAU 1985 recommended value $R_0$ = 8.5 kpc while $\Theta_0$ = 236±7 km s$^{-1}$ of [36] is larger than the IAU 1985 recommended value $\Theta_0$ = 220 km s$^{-1}$. These indicate that the total mass of the Milky Way is ∼10-30% is heavier than previously thought. This is because the total mass ($M$) of the Milky Way scales as $M \propto (\Theta_0)^3$ if we assume the NFW dark halo [27].

Reid et al. [36] and VERA Collaboration et al. [45] reported the modest correlation between $R_0$ and $\Theta_0$ with $r_{R_0,\Theta_0} = 0.45$. Since Reid et al. [36] found correlations between $\Theta_0$ and other model parameters, they needed appropriate priors for some of those parameters. Quiroga-Nuñez et al. [30] generated mock data which resemble the current VLBI astrometry results and they determined the fundamental Galactic parameters including Galactic constants as Reid et al. [36] and VERA Collaboration et al. [45] conducted. They revealed that the correlation between $R_0$ and $\Theta_0$ depends on the range and distribution of parallax results. Thus, parallax measurements from a VLBI array in the southern hemisphere are needed to reduce the correlation.

### 3.2 An accretion event in a high-mass protostar

The maser monitoring organization (M2O[6]) consisting of more than 80 astronomers/observers/theorists is a global community for maser-driven astronomy, which aims to better understand the nature of astrophysical masers, their flaring behavior and their uses as tracers of astrophysical phenomena.

[3]The background image of Fig. 2 can be downloaded from https://astronomy.nju.edu.cn/xtzl/EN/index.html

[4]The web page of the VERA project: https://www.miz.nao.ac.jp/veraserver/

[5]The web page of the BeSSeL project: http://bessel.vlbi-astrometry.org/home

[6]The web page of the M2O: https://www.masermonitoring.com/

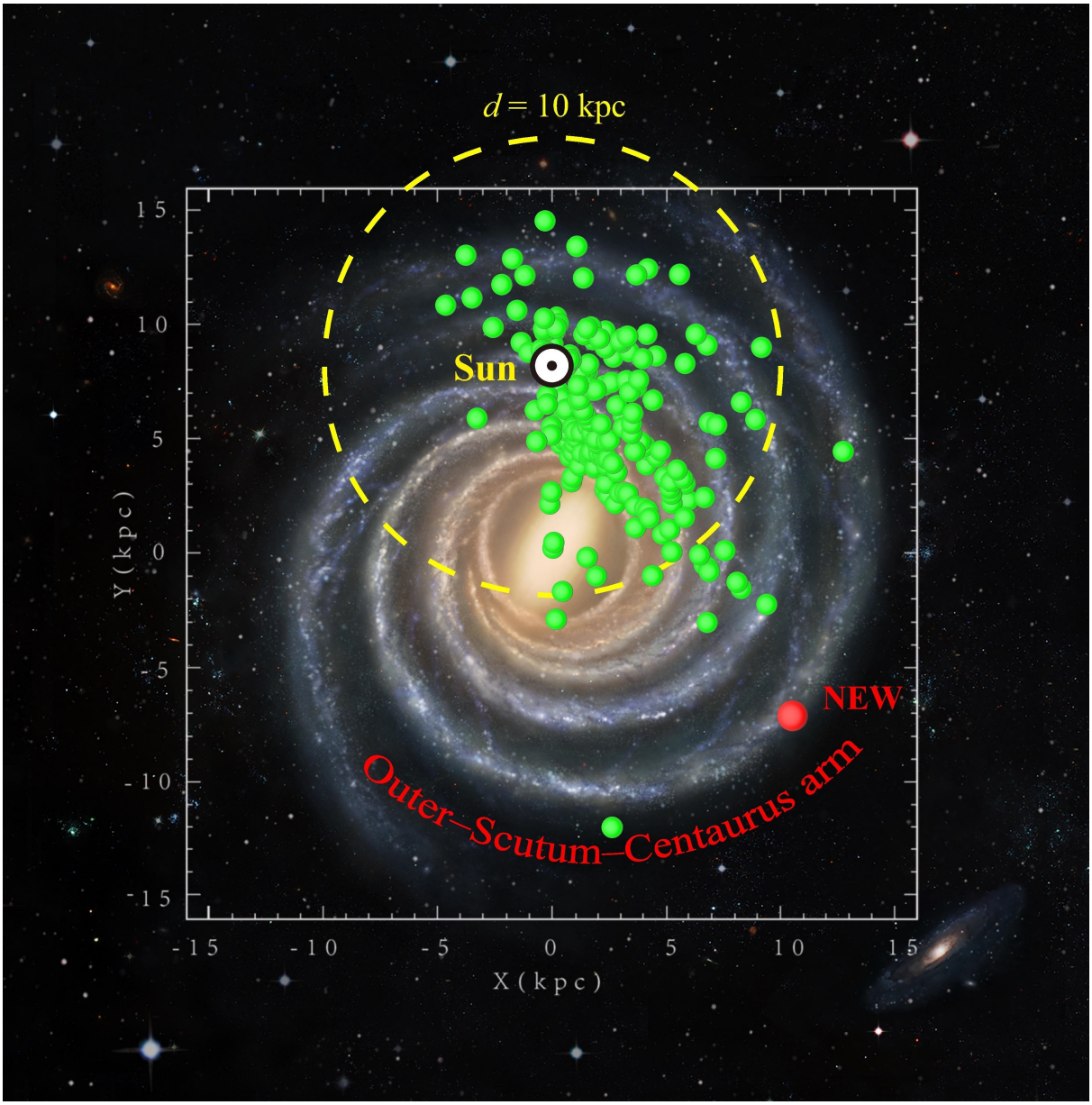


**Figure 2:** *Sakai et al. [38] (edited)*: The most scientifically accurate visualization of the Milky Way (at the moment) on which ~200 VLBI astrometric results (green circles; Reid et al. [36]; VERA Collaboration et al. [45]) are superimposed. The visualization was conducted by a combination of computer and handwork by the BeSSeL project. To paint a realistic image, the component elements of spiral arms were considered such as young OB stars, giant H II regions, young star clusters, nebulas and filaments based on the images of a variety of spiral galaxies. The Milky Way is a four-arm spiral with extra arm segments and spurs. The astrometric result of G034.84−00.95 is emphasized by the red circle. The source is associated with the Outer-Scutum-Centaurus arm. Yellow dashed circle shows a distance of 10 kpc from the Sun within which most astrometric results are distributed. **(Image Credit**[3]**)**©Xingwu Zheng & Mark Reid, BeSSeL/NJU/CfA.

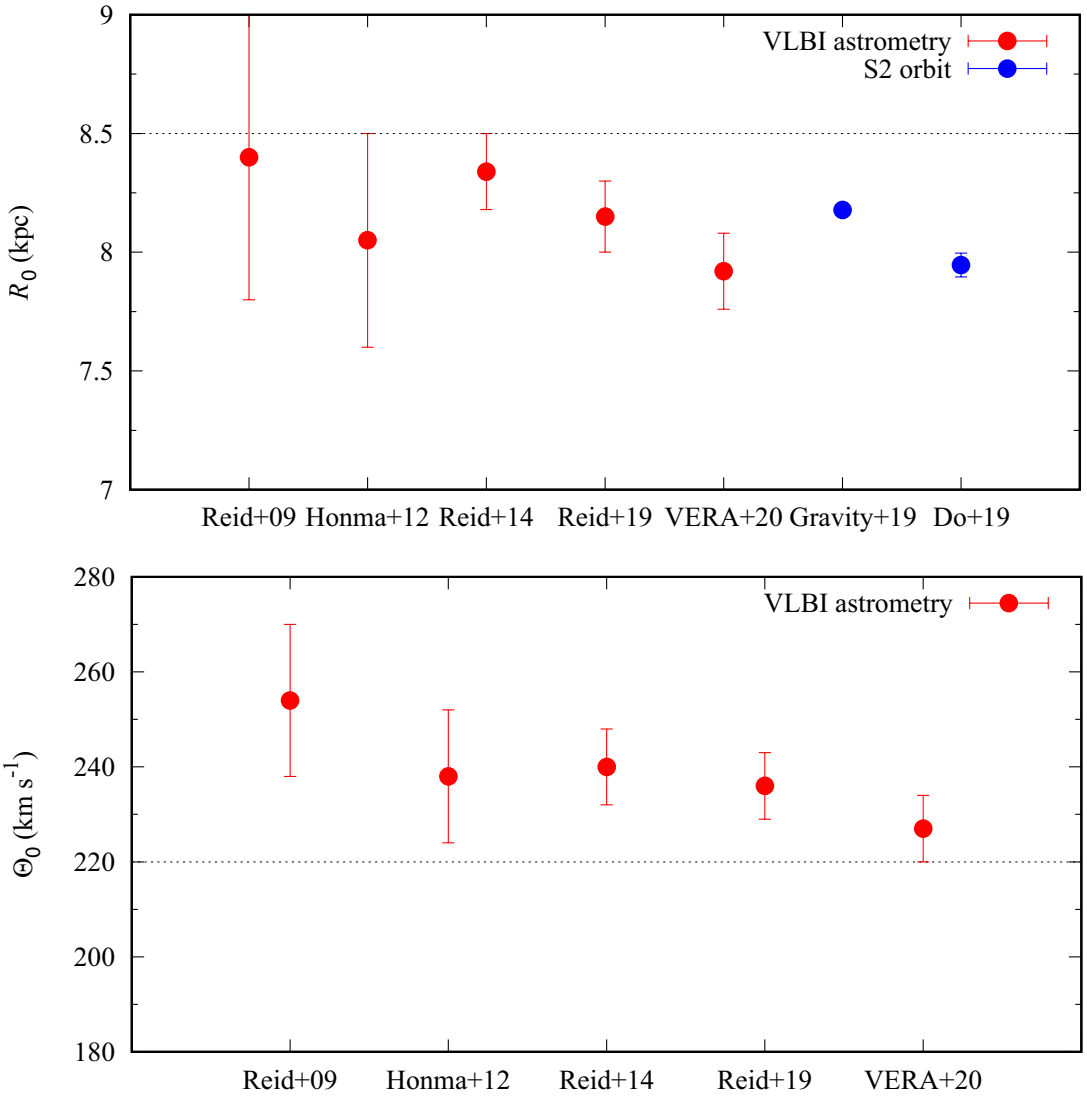


**Figure 3:** The determination of Galactic constants which are $R_0$ (**Top panel**) and $\Theta_0$ (**Bottom panel**). Different colors distinguish methods used for the determination of ($R_0$, $\Theta_0$). Error bars represent only statistical errors. Dashed horizontal lines in both plots display IAU 1985 recommended values of $R_0$ = 8.5 kpc and $\Theta_0$ = 220 km s$^{-1}$ [20]. The horizontal axis in each plot shows references (i.e., Reid+09 = 34; Honma+12 = 15; Reid+14 = 35; Reid+19 = 36; VERA+20 = 45; Gravity+19 = 12; Do+19 = 8).

Nineteen scientific papers have been published by M2O since 2019, among which two papers were published from a *Nature* journal *"Nature Astronomy"* (4; 5). One of the *Nature Astronomy* papers, Burns et al. [4], showed a good example of M2O science. A flare of 6.7-GHz methanol maser was identified for the high-mass protostar G358.93−0.03-MM1 (hereafter "G358-MM1") by monitoring observations with Hitachi 32m radio telescope [41]. While masers can be used to investigate accretion bursts (16; 22; 24; 42), the 6.7-GHz methanol maser arises in the existence of far-infrared radiation from warm dust (>100 K) and high gas densities ($10^{5-8}$ cm$^{-3}$; 6). Thus, the 6.7-GHz maser can be used to investigate the star-formation process in a high-mass protostar.

Followed by the 6.7-GHz methanol maser flare in G358-MM1, multi-wavelength intensive monitoring and follow-up observations were conducted for the same source with the Submillimeter Array, the Atacama Large Millimeter/submillimeter Array (ALMA), the Australian Telescope Compact Array (ATCA), the Southern Hemisphere Long Baseline Array (LBA), the NSF's Karl G. Jansky Very Large Array, and the Stratospheric Observatory for Infrared Astronomy (SOFIA). Based on observations conducted before (the Hi-GAL survey; 23) and after (SOFIA) the maser burst, the flux density of G358-MM1 at 160 $\mu$m was roughly increased three times from 111.7±0.7 Jy to 295.7±13.7 Jy during the bursting phase. The observational results verified the occurrence of an accretion burst in G358-MM1.

Two epochs 6.7-GHz LBA observations allowed the M2O members to measure the proper motion of G358-MM1 to be 1-2 milliarcsecond day$^{-1}$ corresponding to 11,700 - 23,400 km s$^{-1}$ (4-8 % of the speed of light) at a source distance of 6.75 kpc. Such a fast motion cannot be attributed to the physical motions of methanol gas clouds since the gas phase abundance of methanol gas is low in the presence of shocks faster than 10 km s$^{-1}$ [11].

All the observational results described above can be explained by the hypothesis of an accretion event in which enhanced far-infrared radiation drives the production of 6.7-GHz methanol masers. Thermal energy is transferred by photons which is scattered, absorbed and re-emitted by dust grains. This leads to subluminal propagation of the radiation required to produce the maser emission. The phenomenon is recognized as the propagation of a thermal radiation "heat wave".

Three cases of the maser burst have been reported for G358-MM1, S255IR-NIRS3, and NGC6334I. The maser burst of G358-MM1 exhibited a quicker rise and decline compared to the other sources, which indicates a wide variety of maser accretion bursts in a high-mass protostar. Further investigations of the maser accretion bursts are important to better understand the star-formation process in a high-mass protostar.

## 4. Future prospects

### 4.1 Revealing the structure of the Extreme Outer Galaxy with maser astrometry

Current VLBI parallax results are limited within 10 kpc from the Sun, which is not enough to map the whole structure of the Milky Way. Optical astrometry using *Gaia* is not transparent toward the Galactic disk. Thus, VLBI astrometry for sources whose distances are greater than 10 kpc is important to reveal the whole structure of the Milky Way.

The Extreme Outer Galaxy (EOG) is defined as the region outside the Outer spiral arm or at a Galactocentric distance $R \geq 2R_0$ where $R_0$ is the Galactocentric distance to the Sun [7]. Sakai et al. [38] conducted VLBI astrometry using the KaVA (KVN and VERA array) toward the Outer-Scutum-Centaurus arm which is located in an EOG region. They observed a 22 GHz water maser source which is associated with a high-mass star forming region G034.84−00.95. They determined

a source distance of 18.6±1.0 kpc based on both the line-of-sight velocity and the proper motion component in the direction of Galactic longitude. This type of distance is called 2D kinematic distance which is more accurate than the conventional kinematic distance (i.e., 1D kinematic distance). The source is superimposed on a scientifically accurate map of the Milky Way in Fig. 2 (see red circle in the figure).

Reid [31] conducted a simulation study and concluded that 2D/3D kinematic distances are more accurate than can be achieved with parallax measurements especially for distant sources which are well past the Galactic center. For example, Yamauchi et al. [48] measured the proper motion of G007.47+00.06 with VERA (VLBI Exploration of Radio Astrometry), and estimated a 2D kinematic distance of 20 ± 2 kpc . Sanna et al. [39] confirmed the validity of the 2D kinematic distance via a trigonometric parallax distance measurement of the same source, which was derived to be $20.4^{+2.8}_{-2.2}$ kpc with VLBA (Very Long Baseline Array).

Trigonometric parallax measurements as well as determinations of 2D/3D kinematic distances via measurements of the proper motion will be important to understand the structure of the Extreme Outer Galaxy.

### 4.2 RANGD project led by NARIT

The RANGD is "Radio Astronomy Network and Geodesy for Development at NARIT", which is a national project in Thailand and led by NARIT (National Astronomical Research Institute of Thailand, Public Organization). The project was officially initiated in 2016 and will operate the Thai National Radio Telescope (TNRT) with a diameter of 40 m and two VGOS telescopes with each diameter of 13 m for radio astronomy and geodesy.

TNRT is planned to cover a wide frequency range between 0.3 and 115 GHz with receivers of L/C/X/Ku/K/Q/W bands. Science cases with TNRT are summarized in Jaroenjittichai et al. [19], which includes "Pulsars and Fast Radio Bursts (FRBs)", "Star Forming Regions (SFRs)", "Galaxy and Active Galactic Nuclei (AGNs)", "Evolved Stars", "Radio Emission of Chemically Peculiar (CP) Stars", and "Geodesy". TNRT can be used not only for single-dish observations, but also for VLBI observations by collaborating with existing VLBI arrays such as East Asian VLBI Network (EAVN), Australia Long Baseline Array (LBA), and European VLBI Network (EVN).

The commissioning of TNRT has started in the middle of 2022, and initial scientific operation in L-band and K-band will be conducted from 2023. A new VLBI station in Southeast Asia will be able to improve the *uv*-coverage of the existing VLBI arrays and to strengthen scientific outputs including maser astrometry thanks to better imaging quality.

## Acknowledgments

We thank Phrudth Jaroenjittichai, Koichiro Sugiyama, Apichat Leckngam, and Wiphu Rujopakarn for carefully checking the contents about the RANGD project (i.e., subsection 4.2).

## References

[1] Akahori, T., Imai, H., Eie, S., et al. 2021, VLBI Future Planning Working Group Review Report, VLBI Future Planning Working Group Review Report, June 2021, 4th Edition

[2] Bailer-Jones, C. A. L. 2015, PASP, 127, 994

[3] Bessel, F. W. 1838, MNRAS, 4, 152

[4] Burns, R. A., Sugiyama, K., Hirota, T., et al. 2020, Nature Astronomy, 4, 506

[5] Chen, X., Sobolev, A. M., Ren, Z.-Y., et al. 2020, Nature Astronomy, 4, 1170

[6] Cragg, D. M., Sobolev, A. M., & Godfrey, P. D. 2005, MNRAS, 360, 533

[7] Digel, S., de Geus, E., & Thaddeus, P. 1994, ApJ, 422, 92

[8] Do, T., Hees, A., Ghez, A., et al. 2019, Science, 365, 664

[9] ESA. 1997, ESA Special Publication, 1200, ISBN: 9290923997

[10] Gaia Collaboration, Prusti, T., de Bruijne, J. H. J., et al. 2016, A&A, 595, A1

[11] Garay, G., Mardones, D., Rodríguez, L. F., Caselli, P., & Bourke, T. L. 2002, ApJ, 567, 980

[12] GRAVITY Collaboration, Abuter, R., Amorim, A., et al. 2019, A&A, 625, L10

[13] Hirota, T., Bushimata, T., Choi, Y. K., et al. 2007, PASJ, 59, 897

[14] Honma, M., Bushimata, T., Choi, Y. K., et al. 2007, PASJ, 59, 889

[15] Honma, M., Nagayama, T., Ando, K., et al. 2012, PASJ, 64, 136

[16] Hunter, T. R., Brogan, C. L., MacLeod, G. C., et al. 2018, ApJ, 854, 170

[17] Hyland, L. J., Reid, M. J., Ellingsen, S. P., et al. 2022, ApJ, 932, 52

[18] Hyland, L. J., Reid, M. J., Orosz, G., et al. 2022, arXiv e-prints, arXiv:2212.03555

[19] Jaroenjittichai, P., Sugiyama, K., Kramer, B. H., et al. 2022, arXiv e-prints, arXiv:2210.04926

[20] Kerr, F. J., & Lynden-Bell, D. 1986, MNRAS, 221, 1023

[21] Lutz, T. E., & Kelker, D. H. 1973, PASP, 85, 573

[22] MacLeod, G. C., Smits, D. P., Goedhart, S., et al. 2018, MNRAS, 478, 1077

[23] Molinari, S., Schisano, E., Elia, D., et al. 2016, A&A, 591, A149

[24] Moscadelli, L., Sanna, A., Goddi, C., et al. 2017, A&A, 600, L8

[25] Nagayama, T., Kobayashi, H., Omodaka, T., et al. 2015, PASJ, 67, 65

[26] Nagayama, T., Kobayashi, H., Hirota, T., et al. 2020, PASJ, 72, 52

[27] Navarro, J. F., Frenk, C. S., & White, S. D. M. 1996, ApJ, 462, 563

[28] Perryman, M. A. C. 1989, Nature, 340, 111

[29] Quiroga-Nuñez, L. H., Intema, H. T., Callingham, J. R., et al. 2020, &, 633, A130

[30] Quiroga-Nuñez, L. H., van Langevelde, H. J., Reid, M. J., & Green, J. A. 2017, A&A, 604, A72

[31] Reid, M. J. 2022, AJ, 164, 133

[32] Reid, M. J., & Honma, M. 2014, ARA&A, 52, 339

[33] Reid, M. J., & Menten, K. M. 2020, Astronomische Nachrichten, 341, 860

[34] Reid, M. J., Menten, K. M., Zheng, X. W., et al. 2009, ApJ, 700, 137

[35] Reid, M. J., Menten, K. M., Brunthaler, A., et al. 2014, ApJ, 783, 130

[36] —. 2019, ApJ, 885, 131

[37] Rioja, M. J., & Dodson, R. 2020, A&A Rv, 28, 6

[38] Sakai, N., Zhang, B., Xu, S., et al. 2022, arXiv e-prints, arXiv:2211.12534

[39] Sanna, A., Reid, M. J., Dame, T. M., Menten, K. M., & Brunthaler, A. 2017, Science, 358, 227

[40] Sato, M., Reid, M. J., Brunthaler, A., & Menten, K. M. 2010, ApJ, 720, 1055

[41] Sugiyama, K., Saito, Y., Yonekura, Y., & Momose, M. 2019, The Astronomer's Telegram, 12446, 1

[42] Szymczak, M., Olech, M., Wolak, P., Gérard, E., & Bartkiewicz, A. 2018, A&A, 617, A80

[43] Thompson, A. R., Moran, J. M., & Swenson, George W., J. 2017, Interferometry and Synthesis in Radio Astronomy, 3rd Edition, doi:10.1007/978-3-319-44431-4

[44] van Leeuwen, F. 2007, A&A, 474, 653

[45] VERA Collaboration, Hirota, T., Nagayama, T., et al. 2020, PASJ, 72, 50

[46] Vlemmings, W. H. T., van Langevelde, H. J., Diamond, P. J., Habing, H. J., & Schilizzi, R. T. 2003, A&A, 407, 213

[47] Xu, S., Zhang, B., Reid, M. J., Zheng, X., & Wang, G. 2019, , 875, 114

[48] Yamauchi, A., Yamashita, K., Honma, M., et al. 2016, PASJ, 68, 60

[49] Yu, B., Zijlstra, A., & Jiang, B. 2021, Universe, 7, 119

## 5. Appendix

Based on Akahori et al. [1], approximate formula for the parallax error ($\sigma_\pi$) can be expressed as

$$\sigma_\pi \approx \frac{\sigma_p}{\sqrt{N}} \tag{3}$$

where $N$ is the number of observations and $\sigma_p$ is the single-epoch position error. Note that observations should be conducted to be near the parallax maximum and minimum for satisfying Eq. 3.

Analytic formula for the proper motion error ($\sigma_\mu$) should be consistent with the error of the slope on a straight line as

$$\sigma_\mu = \sigma_p \sqrt{\frac{N}{N\sum t_i^2 - (\sum t_i)^2}} = \sigma_p \sqrt{\frac{1}{\sum t_i^2 - N(\sum t_i/N)^2}}. \tag{4}$$

Here, $t$ is the observation period, $\sum t_i/N$ is the mean value, and $\sum t_i/N = \frac{t}{2}(1+\frac{1}{N})$ if observations are conducted with an equal interval $\Delta t = t/N$. We rewrite Eq. 4 using $\sum t_i/N = \frac{t}{2}(1+\frac{1}{N})$ as

$$\sigma_\mu = \sigma_p \sqrt{\frac{1}{\sum t_i^2 - \frac{Nt^2}{4}(1 + 2/N + 1/N^2)}}. \tag{5}$$

By using the Faulhaber's formula (i.e., $S_2(N) = 1/6{\times}N(N{+}1)(2N{+}1)$) and the equal interval (i.e., $\Delta t = t/N$), the denominator of Eq. 5 can be written as

$$\begin{aligned}
\sum t_i^2 - \frac{Nt^2}{4}(1 + 2/N + 1/N^2) &= \sum (1^2 + 2^2 + 3^2, ..., +N^2)(\Delta t)^2 - \frac{Nt^2}{4}(1 + 2/N + 1/N^2) \\
&= \frac{N(N+1)(2N+1)}{6}(t/N)^2 - \frac{Nt^2}{4}(1 + 2/N + 1/N^2) \\
&= (\frac{1}{12} - \frac{1}{12N^2})Nt^2 \\
&\approx \frac{Nt^2}{12} \text{ for } N \gg 1
\end{aligned} \tag{6}$$

Approximate formula for the proper motion error can be written by substituting Eq. 6 for Eq. 5 as

$$\sigma_\mu \approx \sigma_p \sqrt{\frac{12}{Nt^2}}.$$